OPTIMAL CONTROL APPLICATIONS AND METHODS
Optim. Control Appl. Meth. 2011; **32**:215–238
Published online 17 September 2010 in Wiley Online Library (wileyonlinelibrary.com). DOI: 10.1002/oca.963

Robust servo control of a novel type 1 diabetic model

L. Kovács[1,*,†], B. Kulcsár[2], A. György[1] and Z. Benyó[1]

[1]*Department of Control Engineering and Information Technology, Budapest University of Technology and Economics, H-1117, Magyar tudósok krt. 2., Budapest, Hungary*
[2]*Department of Signals and Systems, Chalmers University of Technology, SE 412-96, Gothenburg, Sweden*

SUMMARY

Robust servo control of a model-based biomedical application is presented in the article. The glucose–insulin control of type 1 diabetic patients is considered to be solved using the results of post-modern robust control principles.

The paper uses a recently published glucose–insulin model and presents the transformation of the model to describe the dynamics of type 1 diabetes mellitus. The nonlinear plant is then linearized at a given steady state point. In order to characterize the uncertainty around the nominal model in frequency domain, a parametric nonlinear model sensitivity analysis is performed using gridding method. The aim of the paper is to underline the viability of the robust servo, linear μ-control algorithm tested in highly nonlinear closed-loop simulation environment. Using two degree-of-freedom robust controller, the structured singular value of the closed-loop is designed to fulfill the robust performance requirements and assure glucose level control.

Glucose level tracking is ensured under simulated and realistic exogenous meal disturbances.

Received 7 April 2009; Revised 6 July 2010; Accepted 15 July 2010

KEY WORDS: type 1 diabetes; robust control; μ-synthesis; glucose tracking; uncertainty

1. INTRODUCTION

The normal blood glucose concentration level in the human body varies in a narrow range (80–120 mg/dl). Diabetes appears if for some reason the human body is unable to control the normal glucose–insulin interaction (e.g. the glucose concentration level is constantly out of the above-mentioned range). Consequences of diabetes are diverse and mostly long term (e.g. increased risk of cardiovascular diseases, neuropathy, and retinopathy [1]).

1.1. Motivation

In many biomedical systems external controller provides the necessary input because the human body could not ensure it. For instance, diabetes is one of the most serious diseases that need to be artificially regulated. The newest statistics of the World Health Organization (WHO) prognosticates more than 1% increase of diabetic patients from 2000 to 2025 and predicts that 5.4% of the adult society will suffer from it by the year 2025 [2]. This warns that due to stress and unhealthy lifestyle diabetes could be the 'disease of the future' (especially in developing countries). In Hungary, about 5–6% of the total population is estimated to suffer from diabetes [3].

*Correspondence to: L. Kovács, Department of Control Engineering and Information Technology, Budapest University of Technology and Economics, H-1117, Magyar tudósok krt. 2., Budapest, Hungary.
†E-mail: lkovacs@iit.bme.hu

Among the four types of diabetes (type 1 or insulin-dependent diabetes mellitus (IDDM), type 2 or insulin-independent diabetes mellitus (IIDM), gestational diabetes, and other special types, like genetic deflections), type 1 can be characterized as a standard clinical picture: the β cells responsible for insulin production are completely destroyed. Accordingly, there is no human insulin production and artificial insulin source has to be applied.

The treatment of diabetes could be controlled by an outer loop, replacing the human glucose–insulin equilibrium system, if needed. The replacement, the outer control might be partially or fully automatized. Self-regulation has several strict requirements, but once it has been designed it permits not only to facilitate the patient's life suffering from the disease, but also using different optimization techniques to optimize the amount of insulin dosage to be injected.

The maintenance of the glucose level, by the appropriate choice of the insulin inlet for a diabetic patient, is currently an active research field in biomedical engineering. This metabolic disorder was lethal until the discovery of insulin in 1921. Nowadays, the life quality of the patients can be enhanced though the disease is still lifelong.

Blood glucose control is one of the most difficult control problems to be solved in biomedical engineering. One of the main reasons is that patients are extremely diverse in their dynamics and, in addition, their characteristics are time varying. The closed-loop glucose regulation, as it was several times formulated [4–7], requires three components:

- glucose sensor,
- insulin pump,
- control algorithm (based on the glucose measurements), which is able to determine the necessary insulin dosage.

The autonomous glucose–insulin control might necessitate a valid mathematical model (a possibly dynamical description) of the type 1 diabetic patient.

1.2. Modeling and control

Modeling the system and controlling its behavior are two tightly connected questions, hence the problems could not be discussed separately. As a result of numerous researches, two main aspects were proposed [7]: model-less (empirical) and model-based approaches.

Model-less approach:

- control algorithm based on curve fitting [8],
- control algorithm based on lookup table [9],
- control algorithm based on rule-based control [10], and
- control algorithm based on PID control [11, 12].

Model-based approach:

- linear [13, 14],
- nonlinear [15–17], and
- comprehensive [18–23].

Model-free or measurement-based algorithms are simple and does not require any additional dynamics. However, the knowledge of the model structure and state variables can be of capital importance when robustness and stability questions are considered. This is the main reason why we focus on the model-based control techniques in the article.

To design an appropriate model-based control an adequate (precise enough) model is necessary. In the last few decades many scientists tried to create mathematical models describing the human blood glucose system. Here we only provide a short overview of the applied techniques and achieved results, a brief overview can be found in [7] and interested readers are invited to consult other dedicated textbooks, e.g. [24, 25].

The mathematical description of the glucose–insulin system of type 1 diabetic patients is usually just an approximation (e.g. the biochemical description in [26]), and consequently it contains neglected static or dynamic components. Furthermore, the model parameters are associated to alternative patients. Therefore, in the paper we take robust control algorithm into account.

DOI: 10.1002/oca

The main contribution of the present work is to show the viability of the robust complex-valued μ-analysis technique in handling autonomous control of type 1 diabetes mellitus. μ-analysis and synthesis tool make use of structuring the predefined uncertainty and by scaling the controller, respectively. The control design procedure is applied for the novel Liu-Tang model [26] transformed to describe type 1 diabetes. Frequency weights are partially taken from the literature, but mostly derived from physiologic concernations and nonlinear model sensitivity analysis.

The paper is organized as follows: first, the novel Liu-Tang model is presented and its control properties are observed. Next, the model transformation for type 1 diabetic description is presented and exemplified by open-loop simulation. The fifth section gives a general overview of the robust control methodology used, which is followed by the sensitivity analysis in frequency domain to determine the nonlinear model uncertainty for control design. Controller design, the explanation of the used weighting functions, the results of the iterations and the simulation results of the obtained controller (on the nonlinear model describing type 1 diabetes mellitus) are presented in Section 6. Finally, conclusions and further research possibilities are formulated.

2. BRIEF REVIEW OF THE NOVEL LIU-TANG MODEL

In contrast with most of the earlier models the model [26] published in 2008 applies a different approach: it considers enzyme activity of glucose–glycogen and glycogen–glucose conversion and glucose utilization dynamics, however, it is not purely a molecular model. Consequently, the cause–effect relations are more plausible, and different functions and processes can be separated. The considered model is approximately halfway from the simplest model of Bergman *et al.* [15] to the extremely complex model of Sorensen [27] with its eight state variables and can be naturally divided into three subsystems: the transition subsystem of glucagon and insulin, the receptor binding subsystem, and the glucose subsystem. Since the model has been published recently and not widely used yet, a brief review is presented here. Parameters can be found in Table I.

2.1. Transition subsystem

It is assumed that plasma insulin does not act directly on glucose metabolism [26], but through cellular insulin [28]. Let x_1 and x_2 denote the concentrations of plasma glucagon and insulin, respectively. Complementing equations of [29] with transition delay of the subsystem, it can be described as

$$\frac{\mathrm{d}x_1}{\mathrm{d}t} = -k^p_{1,1}x_1 - k^p_{1,2}x_1 + w_1, \tag{1}$$

$$\frac{\mathrm{d}x_2}{\mathrm{d}t} = -k^p_{2,1}x_2 - k^p_{2,2}x_2 + w_2, \tag{2}$$

where w_1 and w_2 stand for the concentrations of glucagon and insulin produced by the pancreas—for more-detailed explanation, see Equations (13) and (14).

2.2. Receptor binding subsystem

Let x_3 and x_4 stand for the intracellular concentrations of glucagon and insulin, whereas x_5 and x_6 denote the concentrations of glucagon- and insulin-bound receptors, respectively:

$$\frac{\mathrm{d}x_3}{\mathrm{d}t} = -k^s_{1,1}x_3(R^0_1 - x_5) - k^s_{1,2}x_3 + \frac{k^p_{1,1}x_1V_p}{V}, \tag{3}$$

$$\frac{\mathrm{d}x_4}{\mathrm{d}t} = -k^s_{2,1}x_4(R^0_2 - x_6) - k^s_{2,2}x_4 + \frac{k^p_{2,1}x_2V_p}{V}, \tag{4}$$

$$\frac{\mathrm{d}x_5}{\mathrm{d}t} = k^s_{1,1}x_3(R^0_1 - x_5) - k^r_1x_5, \tag{5}$$

$$\frac{\mathrm{d}x_6}{\mathrm{d}t} = k^s_{2,1}x_4(R^0_2 - x_6) - k^r_2x_6, \tag{6}$$

DOI: 10.1002/oca

Table I. Parameters of the Liu-Tang model.

Parameter	Value	Unit
$k_{1,1}^p$	0.14	min^{-1}
$k_{2,1}^p$	0.14	min^{-1}
$k_{1,2}^p$	0.3	min^{-1}
$k_{2,2}^p$	1/6	min^{-1}
$k_{1,1}^s$	6×10^{7}	$\text{M}^{-1}\text{min}^{-1}$
$k_{2,1}^s$	4.167×10^{-4}	$\text{mU/l}^{-1}\,\text{min}^{-1}$
$k_{1,2}^s$	0.01	min^{-1}
$k_{2,2}^s$	0.01	min^{-1}
k_1^r	0.2	min^{-1}
k_2^r	0.2	min^{-1}
R_1^0	9×10^{-13}	M
R_2^0	0.52	mU/l
$V_{\max}^{gp}$	80	mg/l/min
K_m^{gp}	600	mg/l
$V_{\max}^{gs}$	3.87×10^{-4}	mg/l/min
K_m^{gs}	67.08	mg/l
k_1	8×10^{5}	mU/l^{-1}
k_2	1×10^{-12}	M^{-1}
k_3	4×10^{-12}	M^{-1}
V	11	l
V_p	3	l
U_b	7.2	mg/l/min
U_0	4	mg/l/min
U_m	94	mg/l/min
G_m	2.23×10^{-10}	M/min
R_m	70	mU/l/min
C_1	2000	mg/l
C_2	144	mg/l
C_3	1000	mg/l
C_4	80	mg/l
C_5	1000	mg/l
β	1.77	—
a_1	0.005	mg/l^{-1}
a_2	1/300	mg/l^{-1}
b_1	10	—
b_2	1	—

where R_1^0 and R_2^0 denote the total concentrations of receptors, $k_{j,1}^s$ stand for the hormone-receptor association rates, $k_{j,2}^s$ the degradation rates, and k_j^r the inactivation rates ($j=1,2$). Let V_p denote plasma volume, whereas V is intracellular volume [26].

2.3. Glucose subsystem

Blood glucose has two sources: endogenous hepatic production with glycogen transformation and exogenous meal intake.

DOI: 10.1002/oca

In order to describe glycogen–glucose conversion by the catalytic effect of glycogen phosphorylase and glycogen synthase, Michaelis–Menten equation is used:

$$v^{gp} = \frac{V_{\max}^{gp} x_7}{K_m^{gp} + x_7}, \tag{7}$$

$$v^{gs} = \frac{V_{\max}^{gs} x_8}{K_m^{gs} + x_8}, \tag{8}$$

where x_7 and x_8 denote the glycogen and glucose concentrations, v^{gp} and v^{gs} stand for the reaction rates of glycogen phosphorylase and glycogen synthase, respectively. Let $V_{\max}^{gp}$ and $V_{\max}^{gs}$ denote the maximal reaction rates of the enzymes, whereas K_m^{gp} and K_m^{gs} are their Michaelis–Menten constants. It is assumed that the enzyme activity is proportional to the concentrations of the activated receptors by glucagon and insulin [26].

Exogenous glucose intake is denoted by G_{in}.

Glucose utilization can be divided into two groups: insulin independent (brain and nerve cells) and insulin dependent (muscle and adipose tissues).

Insulin-independent part [30] can be modeled by

$$f_1(x_8) = U_b \left(1 - \mathrm{e}^{-\frac{x_8}{C_2}}\right), \tag{9}$$

where U_b and C_2 are described in Table I.

Insulin-dependent part can be calculated by

$$f_2(x_4, x_8) = \frac{x_8}{C_3}\left[U_0 + \frac{(U_m - U_0)\left(\dfrac{x_4}{C_4}\right)^{\beta}}{1 + \left(\dfrac{x_4}{C_4}\right)^{\beta}}\right], \tag{10}$$

which was originally used in [31] (parameters can be found in Table I).

By modeling glucose–glycogen and glycogen–glucose conversions the glucose subsystem can be described with

$$\frac{\mathrm{d}x_7}{\mathrm{d}t} = \frac{k_1 x_6}{1 + k_2 x_5}\frac{V_{\max}^{gs} x_8}{K_m^{gs} + x_8} - k_3 x_5 \frac{V_{\max}^{gp} x_7}{K_m^{gp} + x_7}, \tag{11}$$

$$\frac{\mathrm{d}x_8}{\mathrm{d}t} = -\frac{k_1 x_6}{1 + k_2 x_5}\frac{V_{\max}^{gs} x_8}{K_m^{gs} + x_8} + k_3 x_5 \frac{V_{\max}^{gp} x_7}{K_m^{gp} + x_7} - f_1(x_8) - f_2(x_4, x_8) + G_{\text{in}}. \tag{12}$$

2.4. Pancreatic control

Hormones of the pancreas have a cardinal role in blood glucose regulation and homeostatic stability since negative feedback of glucagon and insulin through blood glucose level assures controllability (in medical sense):

$$w_1(x_8) = \frac{G_m}{1 + b_1 \mathrm{e}^{a_1(x_8 - C_5)}}, \tag{13}$$

$$w_2(x_8) = \frac{R_m}{1 + b_2 \mathrm{e}^{a_2(C_1 - x_8)}}, \tag{14}$$

where $w_1(x_8)$ and $w_2(x_8)$ denote glucagon release rate (GRR) and insulin release rate (IRR) (total amount of hormones secreted by the pancreas) [29], respectively (GRR and IRR, which was changed for better understanding from GIR and IIR, as in [26]).

DOI: 10.1002/oca

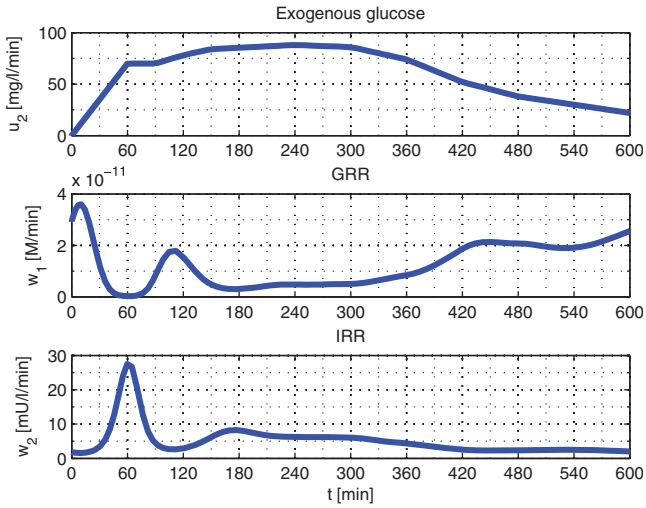

Figure 1. Pancreatic control of the molecular Liu-Tang model [32].

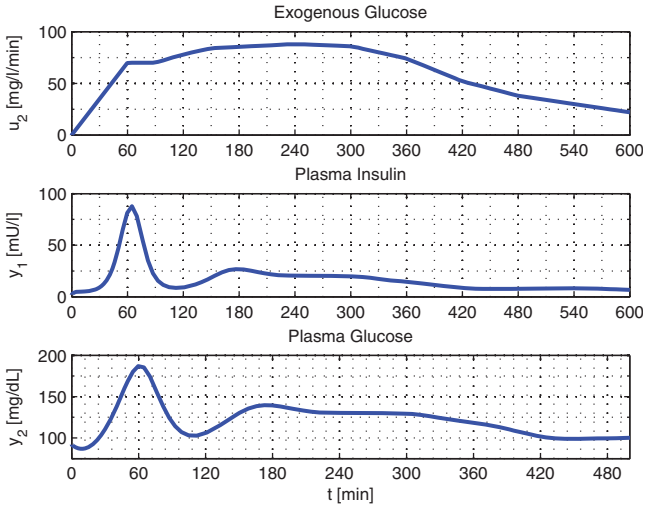

Figure 2. Responses of the Liu-Tang model [32].

Physiologic principles and simulation results are in accordance (see Figures 1 and 2), since elevated glucose concentration results in decrease of GRR and increase of IRR [26]. Healthy range of blood glucose is 80–120 mg/dl (or 800–1200 mg/dl as measurement unit used in [26]), hence below this level glucagon has a key role whereas above insulin takes control.

Remark

The Liu-Tang model [26] uses the mg/l measurement unit, parameters given in Table I are valid for this situation. However, due to the fact that the widely used case for blood glucose level is mg/dl, in the following sections only this is going to be applied.

2.5. Physiologic evaluation

In order to analyze the model in a quantitative manner a physiologically correct exogenous glucose input has to be defined. According to the literature, a widely used [33, 34] absorption curve can be seen in the upper figure of Figure 1, which was recorded under extremely strict and precise

DOI: 10.1002/oca

conditions [32]. It allows us to neglect gut-blood circulation transfer function since it is taken into account by the absorption curve. As we observe healthy system by now, u_1 input of the model is constant zero (no insulin is injected).

Observing the simulation results, it can be seen that the behavior of the system is in accordance with the physiologic expectations: the absorption of exogenous glucose is followed by the activation of the insulin pole (see Figure 1) of the regulatory system (0–50 min). As the main idea of the control mechanism is the dipole structure glucagon secretion of the pancreas increases (see Figure 1) after the insulin phase (50–100 min).

The 'two hump' behavior of the system (see Figure 2) is widely known in medical practice and can be seen here as well: the first intense and short phase of hormone secretion is followed by a long and moderate period assuring rapid reaction and precise correction as well.

3. ASPECT OF CONTROL THEORY

As regards inputs, exogenous insulin (u_1) is completely disposable since it is in daily use in the form of injections (type 1 diabetes is treated in this way). Glucose taken as a meal represents disturbance for the model, but as a result of more profound consideration it can be regarded as the control input for healthy blood glucose household. Consequently, in this section G_{in} is treated as control input, u_2, but in case of type 1 diabetes mellitus it is going to be treated as disturbance.

As for outputs, blood glucose level (x_8) is essential to characterize the system (moreover, it can be measured easily). Concentration of plasma insulin (x_2) is only measurable under laboratory conditions, but any controller designed to regulate pathologic blood glucose system has to be qualified by the amount of injected insulin. Summarizing the considerations, the outputs of the model are plasma insulin (y_1) and blood glucose level (y_2). For physiological validation of the model, plasma insulin is considered here as output in order to analyze the performance of the controller. However, when designing the robust controller, plasma insulin concentration is not used, therefore, it is in accordance with real-life conditions.

The analysis of the model [35, 36] was realized from two aspects: global characteristics were determined by nonlinear analysis [37–39], whereas local properties were observed by steady state linearization [39].

3.1. Nonlinear analysis

As a result of nonlinear analysis based on differential geometry, global control characteristics of the Liu-Tang model are:

- completely reachable, since rank $\Delta^C = 8$, where Δ^C is the reachability distribution,
- number of the observable states of the model is 4, since rank $d\Delta^O = 4$, where $d\Delta^O$ is the observability codistribution,
- static feedback results in such complex vector fields that MATLAB is unable to handle them, hence this question could not be answered this way. Linearization with dynamic feedback (dynamic extension, Cartan fields) has the same problem.

The model is completely reachable, hence every state variable is affected by the inputs [38]. Relevant variables are disposable as outputs, hence partial observability has only theoretical importance. Linearization could not be fulfilled because of the great complexity of the generated vector fields, hence simplification of the nonlinear model is practical.

3.2. Physiological working points

In order to fulfill this, physiologic working points (PWPs) were defined [35, 36]: these are state vectors that are not exact solutions of the differential equations describing the Liu-Tang model, but derived from the normoglycemic steady state [26] by multiplying the values with scaling factors. In this way further LPV (Linear Parameter Varying)-based controller design can be carried out.

DOI: 10.1002/oca

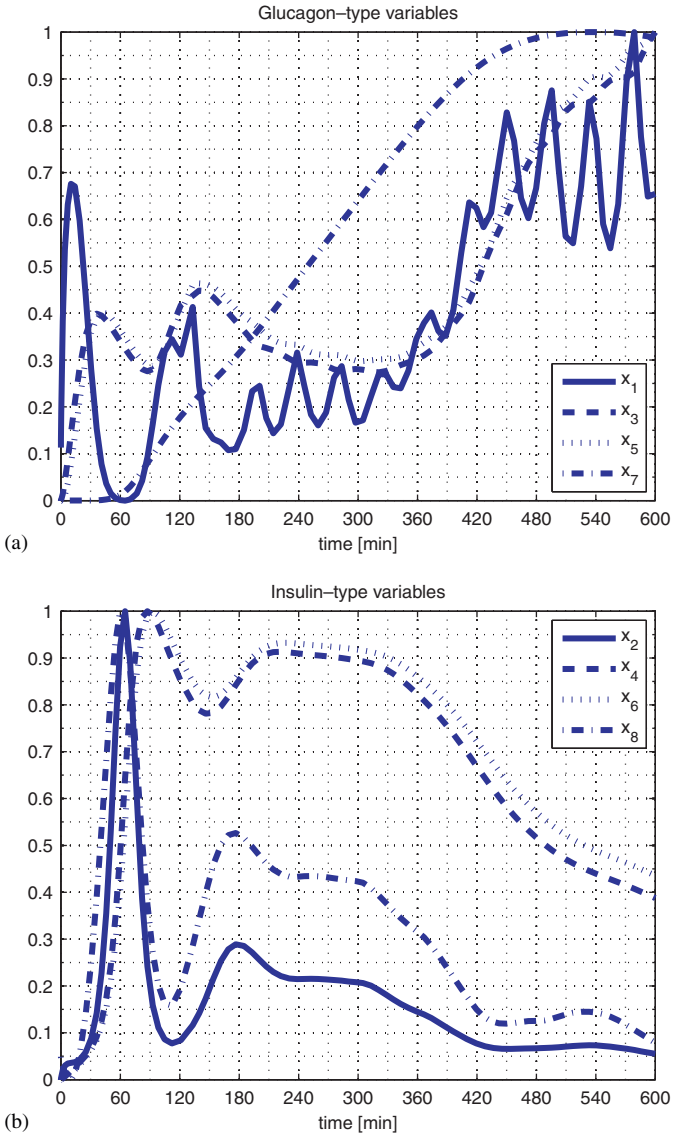

Figure 3. (a) Glucagon- and (b) insulin-type state variables.

Applying only eight different values for each state variable (which is a rather rough quantization) almost 400 000 PWPs should be considered. Exponential explosion is down-to-earth, hence complexity reduction is crucial.

Normalization of the trajectories of the Liu-Tang model to [0,1] results in a valuable experiment: variables can be divided into two groups. One of them is the glucagon-type variables (see Figure 3(a)): plasma glucagon, intracellular glucagon, glucagon-bound receptors, and GRR change together, whereas the other group is the insulin-type variables (see Figure 3(b)), constituted by plasma insulin, intracellular insulin, insulin-bound receptors, glucose, and IRR. Glycogen is the only variable that does not fit perfectly into either group (but can be categorized as an insulin-type variable), which is not surprising, since glycogen is the stored form of glucose that can be interpreted as the integral of the excess glucose (saturation can be remarked after the linear phase).

As a result of biochemical and physiological considerations, variables are divided into two groups: glucagon- and insulin types [35, 36]. PWPs are generated by multiplying the normoglycemic values [26] by [0.25 0.5 0.75 1 1.25 1.5 2 4] in case of both groups, the value of

DOI: 10.1002/oca

glycogen is not modified. The created 64 PWPs are stable, completely controllable, and observable [35, 36].

Intervals of the scaling factors are selected by physiologic considerations: in case of healthy blood glucose household the range of blood glucose level should not excess the range of 50–300 mg/dl, hence the range of observation was set to 25–400 mg/dl. Values of the scaling factors are chosen by varying the resolution: the smaller the blood glucose level, the smaller the resolution. Scaling factors are arbitrarily taken, the main idea in this case was just to cover the physiologic region for the further LPV modeling. The last value (four times the normoglycemic value) is completely unadmittable to be reached in case of type 1 diabetic patients (ketoacidosis state), this value was selected just to ensure that we are covering the physiologic area (and hence the polytopic region of the further LPV model).

3.3. Model reduction

As state variables are connected in a physiological manner, it is probable that the rank of the model can be reduced. In order to perform this, we use state–space transformation and projection.

Let W_c and W_o denote the controllability and observability matrices, respectively, and W_{co} their product. Let T be a transformation, where Λ is diagonal in the factorization

$$W_{co} = T\Lambda T^{-1}. \tag{15}$$

In this manner, the transformed W_c and W_o matrices are

$$\tilde{W}_c = T^{-1} W_c (T^{-1})^*, \tag{16}$$

$$\tilde{W}_o = T^* W_o T, \tag{17}$$

and $\tilde{W}_c = \tilde{W}_o = \Xi$, where Ξ is diagonal [40].

The eigenvalues of the transformed system are the Hankel singular values, and the greater the eigenvalue, the higher the importance of the corresponding state variable. Hankel singular values are $[9.64\ \ 5.89\ \ 1.37\ \ 1.10\ \ 1.38\times10^{-2}\ \ 4.32\times10^{-3}\ \ 7.03\times10^{-5}\ \ 1.31\times10^{-6}]$ for the considered model. It can be seen that the first two eigenvalues are significant, which is expected after the two classes, and after four singular values the others are minor enough to neglect them [36], as it can be also seen in Figure 4, hence second-, fourth- and eight-order models should be observed. Important frequency range is [0.0002 0.2] rad/min [4], so the effect of model reduction was tested with Bode diagrams in frequency domain and with impulse responses in time domain (simulation results for one of the possible four transfer functions can be seen in Figures 5 and 6, the remaining are practically the same) [36]. System with two state variables is quite inaccurate, whereas the approximation is almost perfect with four variables. Mathematical and physiological conclusions are in accordance.

4. MODELING TYPE 1 DIABETES MELLITUS

4.1. Type 1 diabetes mellitus

Type 1 diabetes mellitus, also called insulin-dependent diabetes mellitus or IDDM, is characterized by the loss of insulin producing β cells of pancreas due to an autoimmune process. The lack of insulin and unregulated glucagon production result in elevated blood glucose level and increased osmotic concentration of the blood. In order to restore homeostatic balance, fluid is absorbed from cells and from the interstitial space, consequently, constant thirst, increased fluid intake, and enhanced urine production can be observed. Glucose appears in the urine and the central nervous system senses lack of energy because of glucose burning and provokes hunger, because of meal intake, blood glucose level keeps on increasing [1]. Lipolysis is accelerated in adipose tissues and protein degradation also begins leading to great and rapid loss of body weight. Increased blood density causes declined oxygen supply of tissues, which can result in cerebral hipoxy effecting serious nervous damages.

DOI: 10.1002/oca

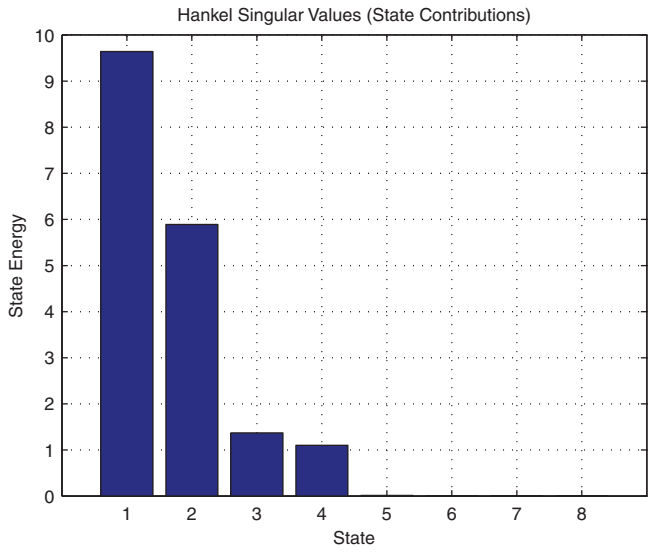

Figure 4. Hankel singular values.

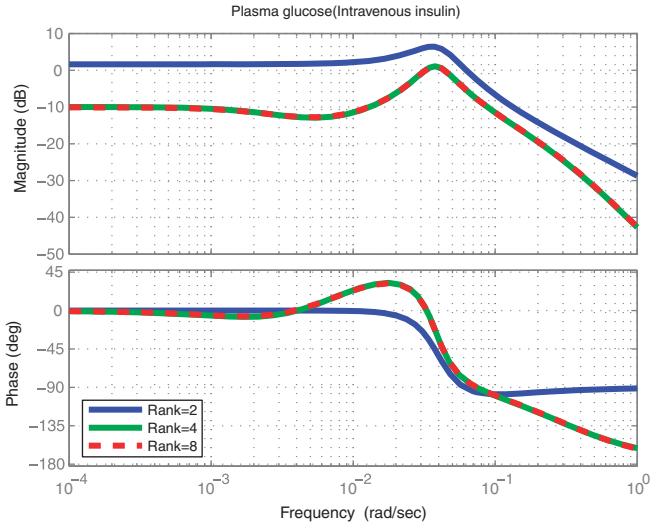

Figure 5. Bode diagrams of plasma glucose (intravenous insulin) transfer functions of the linearized models of different ranks.

Elevated ketogenesis is also a symptom of IDDM which is caused by increased lipolysis. Mediators generated during ketogenesis modify blood pH toward acid region (ketoacidosis) disturbing cell functions and results in puking, increasing fluid loss. Without treatment, coma and death are the final stages of the disease. IDDM is usually diagnosed before the age of 35 with classic clinical symptoms [3].

4.2. Model transformation

The real purpose of the research is to regulate the pathologic system. In order to fulfill this objective, the model has to be transformed to describe type 1 diabetes mellitus.

DOI: 10.1002/oca

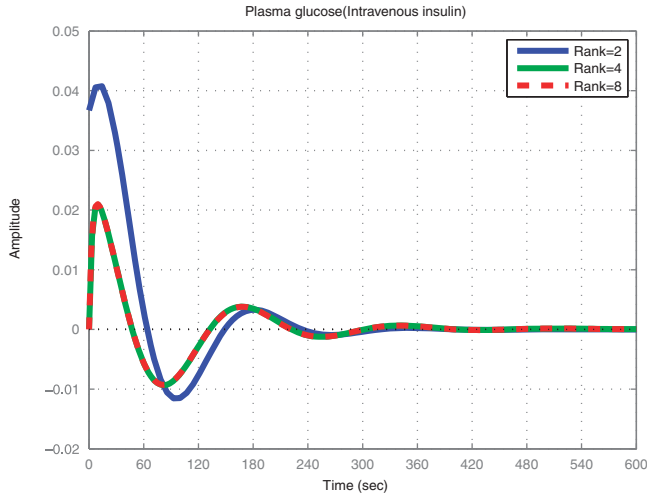

Figure 6. Impulse responses of plasma glucose (intravenous insulin) transfer functions of the linearized models of different ranks.

In case of type 1 diabetes mellitus insulin secretion of the pancreas becomes insufficient to regulate blood glucose. Equation (18) describes the IRR of the pancreas

$$w_2(x_8) = \frac{R_m}{1 + b_2 e^{a_2(C_1 - x_8)}}, \tag{18}$$

where R_m denotes saturation value of pancreatic insulin secretion. In order to model type 1 diabetes mellitus, R_m has to be decreased resulting in unsatisfactory pancreatic insulin secretion.

4.3. Open-loop simulation

By setting $R_m = 0$, type 1 diabetes can be modeled. Applying the glucose input presented in the upper part of Figure 2 [32], open-loop simulation can be realized (see Figure 7). Initial conditions are adapted from [26], where $x_2(0) = 2\,\text{mU/l}$, hence plasma insulin is present at the beginning of the simulation. Observing Figure 7, it can be seen that with no insulin secretion (open-loop simulation, no feedback is applied) blood glucose level elevates for about 360 min to 1500 mg/dl (which is lethal) then decreases as a result of the delayed effect of insulin (by this time plasma insulin is almost zero). Consequently, type 1 diabetes conditions can be created.

5. ROBUST CONTROL DESIGN USING COMPLEX μ-SYNTHESIS

The section briefly summarizes the control methodology applied in the article.

Linear $\mathscr{H}_\infty$ and μ-control synthesis are promising methods on the palette of robust control systems. These postmodern techniques date back to about two decades [41]. Progressively it gains ground by the more and more powerful computational software and hardware [42, 43]. One of the biggest advantages of these methods (beyond the well defined mathematical backgrounds) is the robustness against model mismatches and disturbances. For robust control synthesis, let us consider the augmented system drawn in Figure 8 [44].

Necessary and sufficient conditions of robust stability (RS) and robust performance (RP) can be formulated in terms of the structured singular value denoted as μ [42].

Figure 8 represents the closed-loop system block diagram of the proposed robust servo control problem. The model is denoted by G_n, the controller by K, while the other elements are associated with the uncertainty models and performance objectives considered for the robust control design. As signals r is the reference, u is the control input, y is the output, n is the measurement noise,

DOI: 10.1002/oca

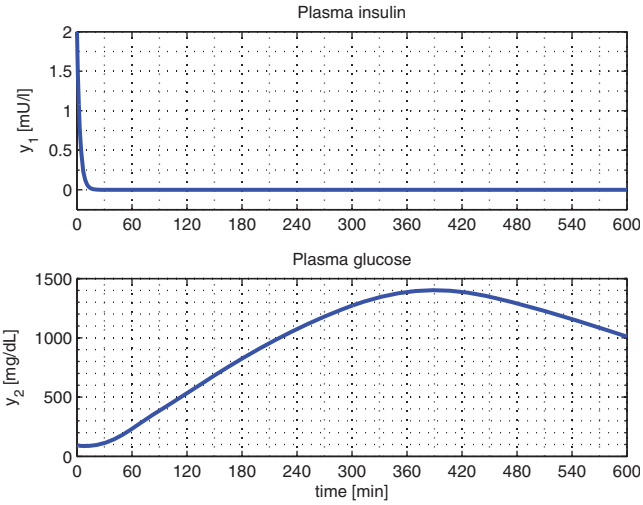

Figure 7. Responses of the transformed Liu-Tang model to type 1 diabetic case.

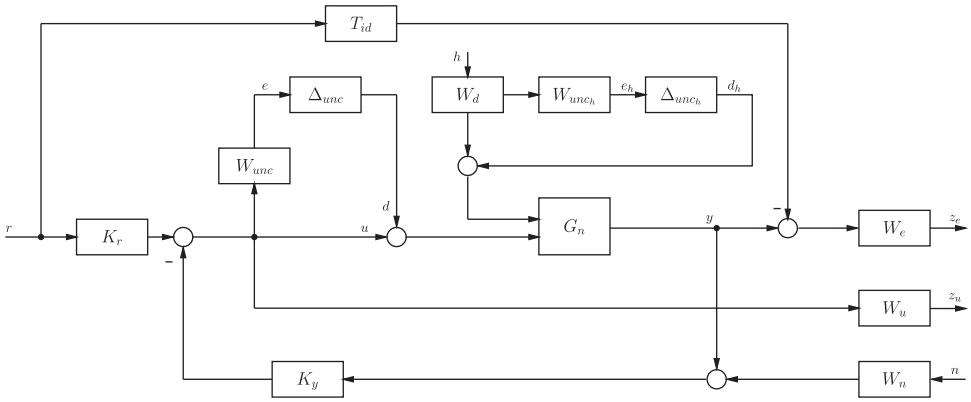

Figure 8. Considered closed-loop interconnection of the proposed robust control problem.

whereas z_e is the deviation of the output from the required one. The structure of the controller K may be partitioned into two parts: $K = [K_r \quad K_y]$, where K_y is the feedback part of the controller and K_r is the pre-filter part. Now the design setup in Figure 8 should be formalized as a standard design problem illustrated in Figure 9.

With the created augmented $P-K$ structure and by introducing the lower linear fractional transformation (LFT) of the pair (P, K), i.e. $M = \mathscr{F}_l(P, K)$, [42], one gets back the $\Delta - M$ structure (see Figure 9). Hence, the robustness and performance analysis of the augmented plant can be fulfilled by the partition blocks of M:

$$F_l(P, K) = P_{11} + P_{12}K(I - P_{22}K)^{-1}P_{21}, \tag{19}$$

$$\left[\begin{array}{c} e \\ \hline \tilde{z} \end{array}\right] = \left[\begin{array}{c|c} M_{11} & M_{12} \\ \hline M_{21} & M_{22} \end{array}\right] \left[\begin{array}{c} d \\ \hline \tilde{w} \end{array}\right]. \tag{20}$$

Assume that the uncertainty block represented by Δ is a member of the bounded subset:

$$\mathbf{B}\boldsymbol{\Delta} = \{\Delta \in \boldsymbol{\Delta} | \overline{\sigma}\{\Delta\} < 1\}, \tag{21}$$

DOI: 10.1002/oca

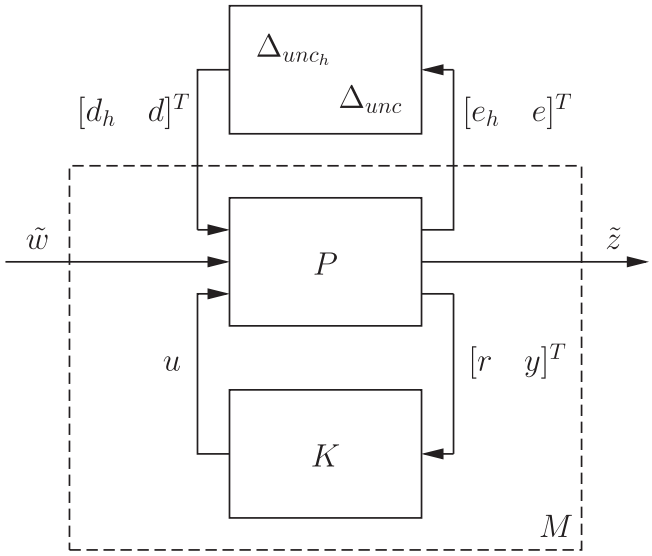

Figure 9. Generalized $\Delta - P - K$ structure.

where $\overline{\sigma}$ represents the largest structured singular value (of the normalized set of structured uncertainties), while $\mathbf{\Delta}$ is defined by

$$\mathbf{\Delta} = \{\text{diag}(\delta_1^c I_{r_1}, \cdots, \delta_{m_c}^c I_{r_{m_c}}, \Delta_1, \cdots, \Delta_n) | \delta_i^c \in \mathbb{C}, \Delta_j \in \mathbb{C}^{m_j \times m_j}\},$$

where the ith repeated complex scalar block is $r_i \times r_i$ and the jth full block is $m_j \times m_j$. The parameters δ_1^c $(i = 1, \ldots, m_c)$ of the repeated scalar blocks can only be real numbers [45].

RS can be guaranteed when the closed-loop system is internally stable. Internal stability means that from all inputs to all outputs the created transfer functions are stable. RS is equivalent to

$$\|M_{11}\|_\infty < 1. \tag{22}$$

The authors restrict the set of perturbation to $\Delta \in \mathbf{B}\mathbf{\Delta}$, therefore, condition (22) might be conservative. A less conservative solution of the problem is to structure uncertainties. This is denoted by the structured singular value μ [42].

The structured singular value can be defined as

$$\mu_{\mathbf{\Delta}}(M) := \frac{1}{\min_\Delta(\overline{\sigma}\{\Delta\} : \Delta \in \mathbf{\Delta}, \det(I - M\Delta) = 0)}, \tag{23}$$

unless no $\Delta \in \mathbf{\Delta}$ makes $I - M\Delta$ singular, in which case $\mu_{\mathbf{\Delta}}(M) = 0$. Thus $1/\mu_{\mathbf{\Delta}}(M)$ is the 'size' of the smallest perturbation Δ, measured by its maximum singular value, which makes $\det(I - M\Delta) = 0$.

From the definition of μ, RS can be reformulated as

$$\sup_\omega \mu(M_{11}) < 1 \Longleftrightarrow \|\mu(M_{11})\|_\infty < 1. \tag{24}$$

The main goal of our synthesis is to guarantee RP. The closed-loop system achieves RP if the performance objective is met:

$$\sup_\omega \mu(M) < 1 \Longleftrightarrow \|\mu(M)\|_\infty < 1. \tag{25}$$

Using μ it is possible to test both RS and RP in a non-conservative manner.

Unfortunately, Equation (25) is not suitable for computing μ, since the implied optimization problem may have multiple local maxima. However, tight upper and lower bounds for μ may be effectively computed for complex perturbation sets. Algorithms for computing these bounds have been documented in several papers [43].

DOI: 10.1002/oca

Define

$$S=\{\text{diag}[D_1,\ldots,D_{m_c},d_1I_{m_1},\ldots,d_nI_{m_{n-1}},I_{m_n}]|D_i\in\mathbb{C}^{r_i\times r_i},D_i=D_i^*>0\},$$

where D_i $(i=1,\ldots,m_c)$ are Hermitian matrices which commute with Δ $(D\Delta D^{-1}=\Delta, D\Delta D^{-1}\in\mathbf{\Delta},\overline{\sigma}(D\Delta D^{-1})=\overline{\sigma}(\Delta))$ [45].

The upper bound can be formulated as a convex optimization problem, hence the global minimum can be found. For a constant matrix M and complex uncertainty structure Δ, an upper bound for $\mu_\Delta(\mathrm{M})$ is

$$\mu_\Delta(M)\leqslant\inf_{D\in S}\overline{\sigma}\{D^{-1}MD\}. \tag{26}$$

The aim of the μ-synthesis is to minimize the peak value of $\mu_\Delta(.)$ of the closed-loop M for all stabilizing controllers K [43].

Using the upper bound, the optimization problem can be formulated as

$$\min_K\sup_\omega\inf_{D(\omega)\in S}\overline{\sigma}\{D^{-1}F_l(P,K)D(\omega)\}. \tag{27}$$

Unfortunately, it is not known how to solve (25). However, an approximation to complex μ-synthesis can be made by the following iterative scheme. For a fixed controller $K(s)$, the problem of finding $D(\omega)$ is just the complex μ upper bound problem, which is a convex problem with known solution. Having found these scaling we may fit stable minimum phase transfer function matrices $D(s)$ to $D(\omega)$ such that the interconnection $D(s)M(s)D(s)^{-1}$ is stable. For given scaling $D(s)$, the problem of finding a controller $K(s)$ minimizing the norm $\|F_l(D(s)M(s)D-1(s),K(s))\|_\infty$ will be reduced to a standard $\mathscr{H}_\infty$ problem. Repeating this procedure (denoted D–K iteration) several times the algorithm converges and the complex μ optimal controller is designed [45].

6. RESULTS

In this section, the robust servo glucose–insulin controller is designed and applied to the model-based diabetic patient system. The nonlinear plant described in the previous section could be linearized at an equilibrium point in order to create a nominal plant for linear μ-synthesis. Both the linear and the nonlinear description are supposed to have two inputs. One of them is the control input and the other is assumed to be disturbance for instant. The control input is the insulin inlet, the disturbance is the glucose intake, whereas the measured quantities are both the plasma insulin and glucose concentrations. The aim of the robust control under model mismatch is the disturbance rejection on the glucose and the tracking of a predefined glucose concentration level reference. During the synthesis one takes the input weighting into account in order to force the designed control input signal to stay in an acceptable magnitude domain, and the controller will be tested on the nonlinear plant with noise-corrupted measurements.

6.1. Uncertainty analysis

Model-based control systems use the mathematical abstraction of the actual plant to be controlled. Although vast identification techniques can be found in the literature, perfect fitting of the model and the real plant do not exist. Therefore, the model (or nominal plant) always contains neglected dynamics of the real world. The nominal plant is usually a lower order system than the real plant, since modeling highly complicated components is very difficult.

One widespread approach of describing uncertainties is the unstructured formulation. Even if the precise uncertainty dynamics is unknown, usually an upper bound could be defined in frequency domain in order to characterize the mismatch. Complex uncertainties, neglected dynamics, respectively, their (frequency depending) bounds could be classified into several groups. Two major types (not counting the more complicated structures) of complex uncertainty could be distinguished: the additive and multiplicative blocks (at the plant output or input for MIMO systems). The choice

DOI: 10.1002/oca

always requires a certain amount of *a priori* information. In case of robust control of T1DM, uncertainty formulation has always been a great challenge: one of the earliest solutions can be found in [4] for the model of Sorensen. Moreover, further improvements of the original idea from a physiological point of view can be found in [22], as well as in [23] for the minimal model of Bergman.

The postmodern control technique, the μ analysis and synthesis, offers to structure the uncertainty around the nominal model by constant or frequency-wise input–output scaling [43, 45]. Thus it might result in a less conservative controller than the pure $\mathscr{H}_\infty$ method. Depending on the nature of the uncertainty (real, complex valued or both) we can distinguish real, complex, and mixed-μ methodologies.

In the current work, we investigate the effectiveness of the complex-valued μ-control synthesis, although we analyze the effect of the model parameter (real valued) *indirectly*. We characterize the multiplicative uncertainty set created by the subsystem parameters around a 'nominal' value. First, we systematically change the parameters in the glucagon, insulin, and the glucose part of the nonlinear model and then we do the linearization with respect to the combination of the new parameter values. Collecting the frequency domain-related information of the linear model, we define the relative uncertainty $U_{\text{rel}}(\omega)$. Finally, re-definition of the model uncertainties might give rise to real- or mixed-valued μ-control synthesis.

In our case (see Figure 8), the input multiplicative uncertainty is preferred, because it specifies the digression, the frequency depending difference (in percentage) between the nominal and actual plants. The uncertainties between the nominal model and the real plant are represented with W_{unc} and Δ_{unc} for the insulin control input part, respectively, W_{unc_h} and Δ_{unc_h} for the disturbance (glucose).

In the following, we neglect the actuator dynamics and high frequency behavior of the nonlinear plant by means of multiplicative description.

Starting from the formal definition of the multiplicative uncertainty

$$M(G_n, W_r) := \left\{ G : \left| \frac{G(i\omega) - G_n(i\omega)}{G_n(i\omega)} \right| \leqslant |W_m r(i\omega)| \right\}, \tag{28}$$

parametric sensitivity was performed on the nonlinear model to determine W_{unc} and W_{unc_h}. The shape of the input multiplicative uncertainty is given in two steps. First, low frequency, i.e. steady state modeling error is determined by sensitivity analysis. Second, the high frequency part is defined to cover neglected nonlinear and actuator dynamics.

The idea was partially adapted and modified from [4]. The idea is to take uncertain parameters in the nonlinear model. Ranges are associated to these selected parameters. By taking every single extremal combination of the parameters, linearization is performed. Finally, the frequency content of the perturbed and linearized model is compared and relative difference is computed. Instead of using the extremal values, hereby a gridding technique is proposed.[‡] Consequently, we consider the combination of the selected parameters in a multiplicative manner (see below). A control-oriented sensitivity test in terms of the rate of the novel model coefficient to the glucose, respectively, to insulin amount (healthy case) is proposed in [26]. However, only a limited number of parameters were analyzed, k_1, k_2, k_3 (for the feedback gains of the model). In case of other models, detailed analysis can be found in [4] and [46].

Due to the fact that no physical data was available (from which to identify ranges of parametric uncertainty), but based on the results of sensitivity analysis of [26] a $\pm 10\%$ variability of the insulin subsystem and a $\pm 10\%$ variability of the glucagon/glucose subsystem were assumed. Here, we suggest to check the sensitivity with respect to $k^p_{1,1}$, $k^p_{1,2}$, $k^p_{2,1}$, $k^p_{2,2}$ (for the plasma transition subsystem), $k^s_{1,1}$, $k^s_{1,2}$, $k^s_{2,1}$, $k^s_{2,2}$ (for the intracellular subsystem), and k_1, k_2, k_3 as well. The sensitivity analysis was performed separately for the insulin part and the glucagon/glucose part. For each parameters a $(+\max, \frac{1}{2}\max, -\frac{1}{2}\max, -\max)$ grid was used to the nominal value.

[‡]The price to pay is increasing number of parameter combination. Moreover, not all of the grid combinations have physical meaning.

DOI: 10.1002/oca

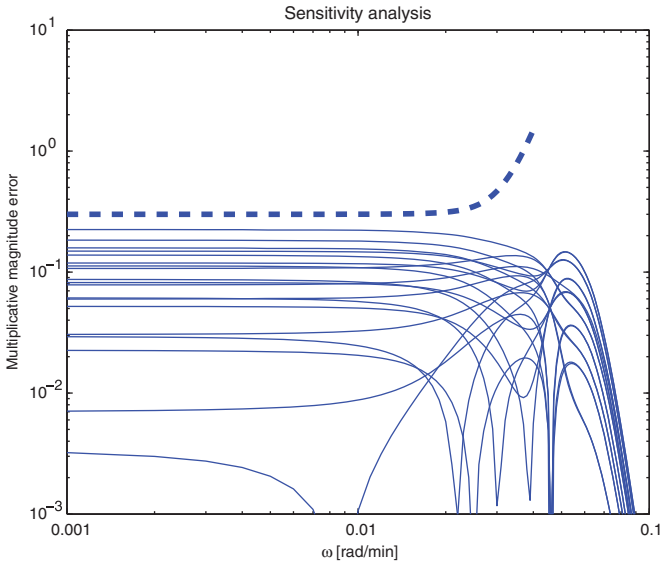

Figure 10. Selected relative modeling error functions in frequency domain (solid lines, for the $\pm 10\%$ variation in $k^p_{i,2}$ as well as in $k^s_{i,j}$, where $i, j = 1, 2$) and the selected uncertainty upperbound (dashed line).

For each possible combination the nonlinear model was linearized and the obtained linear model was used to determine parametric sensitivity by determining sup W_{rel} of the relative uncertainty relation $U_{\text{rel}}(\omega) = |(G_p(\omega) - G(\omega))/G(\omega)|$, where G_p stands for the perturbed model and G for the nominal one. The frequency range of interest was $\omega \in [0.001, 0.1]$ rad/s.

It was observed that the latter three terms do not influence the unhealthy model description. They only have neglectable influence on the input multiplicative uncertainty. On the other hand, $k^p_{i,2}$ as well as $k^s_{i,j}$ (where $i, j = 1, 2$) can be used to characterize the low frequency bound on the input multiplicative uncertainties. The results of the insulin-related part can be seen in Figure 10 (the results are similar for glucagon/glucose part).

As the cross-over frequency of the open-loop linear model is around 1 rad/min, the uncertainty weight in high frequency range is supposed to be over 1, i.e. the nominal model is over 100% inaccurate. No actuator dynamics are considered and supposed to be involved in the uncertainty function.

Consequently, the determined relations for the two uncertainty functions are

$$W_{\text{unc}} = \frac{15}{s^2 + 10.05s + 1}, \tag{29}$$

$$W_{\text{unc}_h} = \frac{5}{s^2 + 10.05s + 1}. \tag{30}$$

The model matching function, T_{id}, generally is an ideal transfer function of the plant. It was selected to react quickly on glucose disturbance and its time constant was synchronized with the Oral Glucose Tolerance Test time interval (120 min).

The control input is limited implicitly (no hard constraint or saturation can be considered in the design phase) and can be highly weighted using a performance criteria W_u. The larger the weight, the smaller the deflections, therefore, the control activity can be reduced. The weight on insulin inlet is defined to be constant over the entire frequency range and with a magnitude equal to the inverse of the maximal quantity. Based on [4], it was demonstrated its maximal value as 38.525 μU/ml. In our case, a stricter constraint was applied, hence we selected a much smaller rate: 10 μU/ml.

DOI: 10.1002/oca

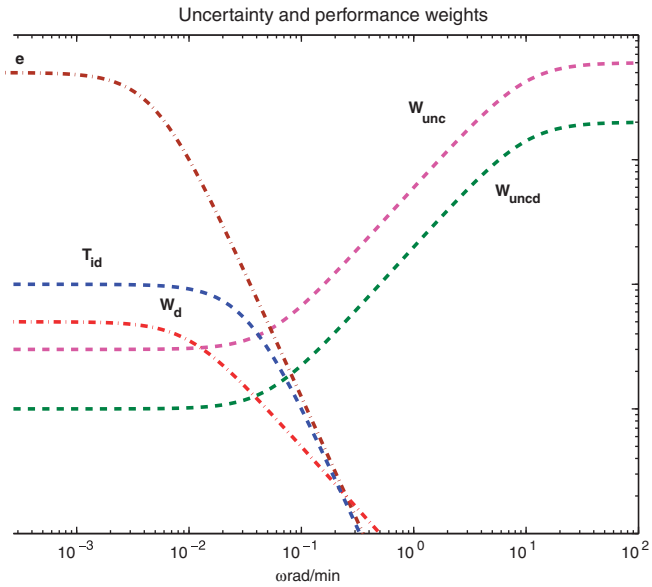

Figure 11. Frequency response of the weighting functions.

The weighting function, W_e, chosen for tracking errors can be thought as penalty function: W_e should be large in frequency range where small errors are desired and small where larger errors can be tolerated. Advisedly, the choice of the weights can be performed. To achieve perfect tracking (i.e. integral action), W_e should be large at very low frequency to imitate integrator. At the same time, good tracking property and nominal model validity can be treated as a trade-off. Uncertain model cannot be forced to assure nominal performance requirements. To assure good tracking performance, W_e was increased at lower frequency up to 50. Therefore, based on the small gain theorem [42], the permitted tracking error in this range is over $0.02\,\mu\text{U/ml}$. More the weight is decreased in frequency, larger the tracking slip is. Uncertain system can not be forced to perfectly follow the reference signal.

The role of the weighted sensor noises, W_n, and external disturbances, W_d, is basically the opposite of the role of weights for output discussed so far. Inputs to the weights are signals whose frequency responses are flat and unit size. The weights themselves contain scale factors and frequency shaping matching the size, unit, and frequency content of the true inputs. The first category consists of simple constants used to model wide-band signals, such as sensor noise W_n. The general percentage of the incorporating noise, by channel, might not be over 2–5%. During the design process, W_n, anticipates 5% measurement noise for both insulin and glucose measurements (values taken from clinical experience) [44]. The second category of disturbance weights consists of low pass filters used to model band-limited signals, such as W_d. Typically, these weights are first-order transfer functions with gains selected to produce the correct signal levels and time constants chosen to match the bandwidth of the signals. In comparison with [4], a sharper transfer function is used:

$$W_d = \frac{0.5}{100s+1}. \tag{31}$$

As a result, Figure 11 captures the frequency plots of the weighting functions discussed above.

6.2. *Controller design*

With the defined weighting functions the augmented closed-loop interconnection (see Figure 8) can be structured in the generalized $\Delta - P - K$ form (see Figure 9), where

$$\tilde{w} = [r \;\; n \;\; h]^{\mathrm{T}}, \;\; \tilde{z} = [z_e \;\;\; z_u]^{\mathrm{T}}. \tag{32}$$

DOI: 10.1002/oca

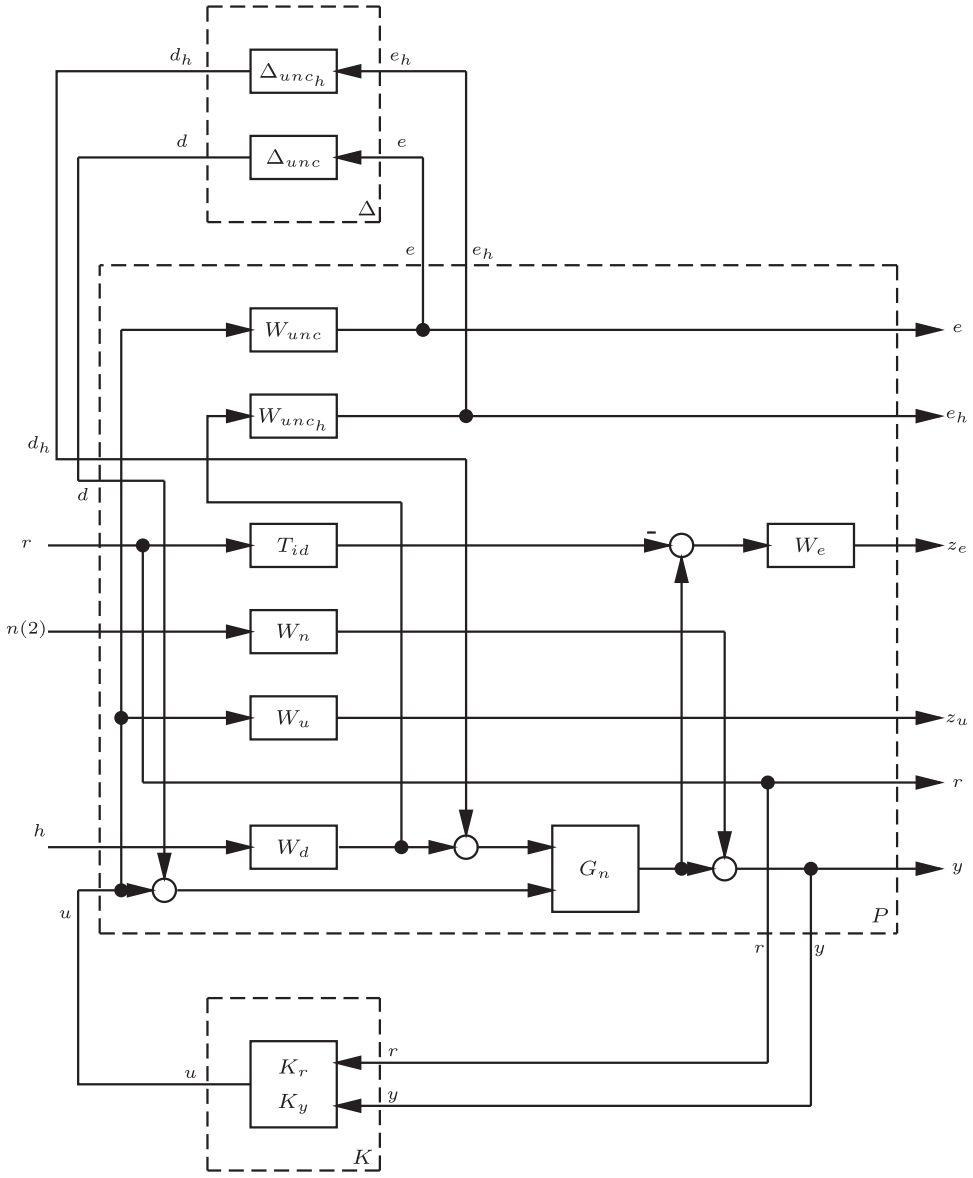

Figure 12. Detailed $\Delta - P - K$ structure.

This can be easily understood by the detailed $\Delta - P - K$ structure presented in Figure 12 and is described as follows:

$$\begin{bmatrix} e \\ e_h \\ z_e \\ z_u \\ r \\ y \end{bmatrix} = \begin{bmatrix} 0 & 0 & 0 & 0 & 0 & W_{\text{unc}} \\ 0 & 0 & 0 & 0 & W_{\text{unc}_h} W_d & 0 \\ W_e G_n^u & -W_e T_{id} & 0 & 0 & W_e G_n^h W_d & W_e G_n^u \\ 0 & 0 & 0 & 0 & 0 & W_u \\ 0 & I & 0 & 0 & 0 & 0 \\ G_n^u & 0 & W_n & W_n & G_n^h W_d & G_n^u \end{bmatrix} \begin{bmatrix} d \\ r \\ n(2) \\ h \\ u \end{bmatrix}. \tag{33}$$

Summarizing the iterative steps obtained by the μ-synthesis (Table II), one can see that by adopting the $\mathscr{H}_\infty$-synthesis method (e.g. γ-iteration) the RP prescription can not be achieved. A

DOI: 10.1002/oca

Table II. Iteration summary.

Iteration	1	2	3
Controller order	15	19	23
D-scale order	0	4	8
γ archived	1.563	1.021	1.006
Peak value of μ	1.480	0.980	0.962

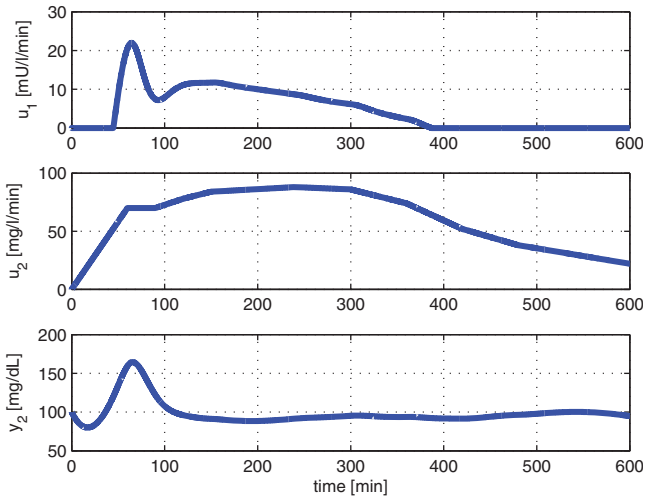

Figure 13. Close-loop responses of the μ-synthesis on the nonlinear model.

less conservative solution might be the μ-synthesis by $D-K$ iteration for complex uncertainty [43]. The final (frequency depending) D scale assures the RS, because the computed and scaled μ-value is under 1. Consequently, RP is met. However, the controller degree increased significantly.

6.3. *Physiologic validation*

Testing the robust servo controller using the food intake presented in the upper part of Figure 2, it can be seen (Figure 13) that the glucose concentration (y_2) stays in the normal 80–120 mg/dl range, while the insulin control input (u_1) is optimized. The glucose concentration is out of the mentioned region (165 mg/dl) only at the beginning of the meal absorbtion (u_2), but this is normal in case of food intake.

Moreover, during the simulation the glucose concentration decreases to 77 mg/dl, which can be explained by the mix of the delay of the insulin effect and the high glucose input, although the mentioned period is near the normal range without reaching the upper bound of hypoglycemia.

6.4. *Virtual validation*

In order to observe the real performance and robustness of the designed controller, several different input data should be used. Given the fact that the required input of the Liu-Tang model is glucose absorption, which is greatly difficult to measure, the only real input data we have is [32]. Therefore, the authors generated virtual but plausible and realistic absorption data.

Based on theoretical models of absorption [47], the concentration of glucose absorbed can be considered to follow a Weibull curve as a function of time:

$$g = p_3 \left(\frac{t}{p_1}\right)^{p_2} \mathrm{e}^{-\left(\frac{t}{p_1}\right)^{p_2}}. \tag{34}$$

DOI: 10.1002/oca

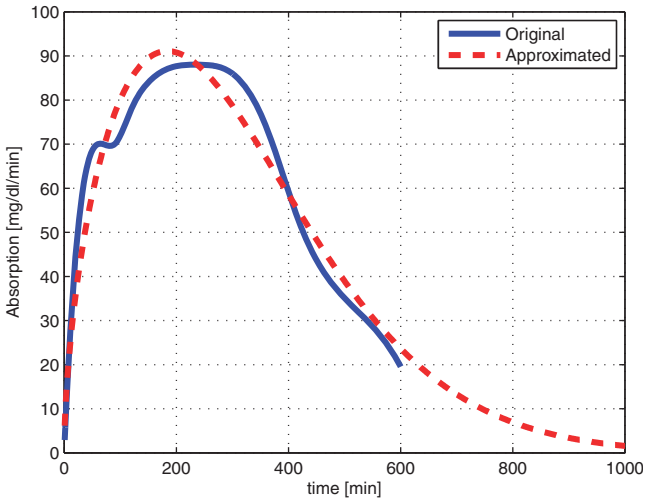

Figure 14. The original absorption curve of [32] and the approximated.

Observing the role of parameters p_1, p_2, and p_3, it can be seen that p_1 corresponds to the input scaling; in other words, it scales the curve along the horizontal axis. Variable p_2 determines the shape of the curve, since it can be interpreted as a time constant of the system, whereas p_3 scales the curve along the vertical axis. Therefore, the amount of the glucose input can be taken into account by p_3, whereas patient variability can be modeled by p_2. It has to be noted that this method is not to create the precise model of glucose absorption (e.g. the exact quantitative relationship between patient variability and p_2; or meal input and p_3 is not determined, although physiological considerations were taken into account) but to generate plausible absorption curves based on [32].

Approximating the absorption curve presented in [32], the following parameters are derived: $p_1 = 344.54$, $p_2 = 1.59$, and $p_3 = 190.49$. The original absorption curve of [32] and the approximated can be seen in Figure 14.

In order to test the robustness of the designed controller, three simulations are presented here:

1. original: $p = [p_1 \ p_2 \ p_3]$,
2. increased amount of input glucose: $p = [p_1 \ p_2 \ 1.5p_3]$,
3. smaller time constant, faster absorption (patient variability): $p = [p_1 \ 0.8p_2 \ p_3]$.

Closed-loop simulation results can be seen in Figures 15–17. Observing glucose levels, it can be seen that the controller is robust enough in terms of meal disturbance and patient variability, since blood glucose level stays in the desired range. However, it has to be remarked that blood glucose level is sometimes near to upper hypoglycemia. In these situations, the controller switches off, no insulin is injected, hence blood glucose level starts to increase. Later, if blood glucose level is getting too high (see Figure 17, after 550 min), the controller switches on again, therefore, blood glucose is regulated by additional insulin injection.

The results are plausible from a physiological aspect, since time delay can be observed between insulin injections and blood glucose level (see Figures 15–17).

7. CONCLUSION

Linear robust μ-synthesis design was applied to assure RP with structuring the uncertainty description of model-based glucose–insulin system. The paper exemplifies the robust control design technique for a useful biomedical application, autonomous type 1 diabetes control. Diabetes mellitus is a very serious disease and its modeling and on-line control is an active research topic nowadays.

DOI: 10.1002/oca

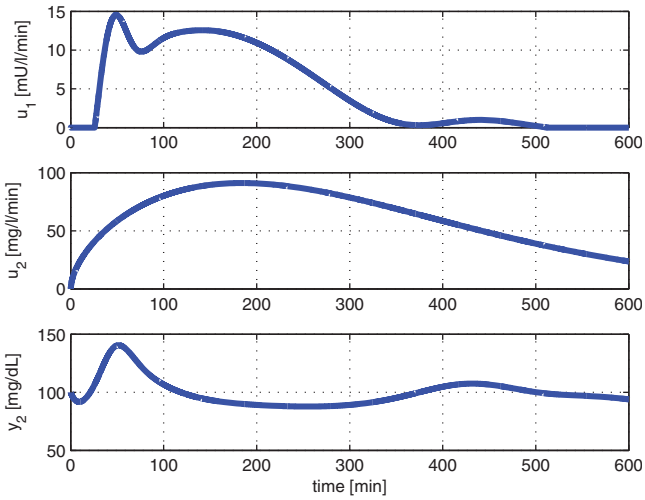

Figure 15. Closed-loop response of the nonlinear model with $p=[p_1 \;\; p_2 \;\; p_3]$.

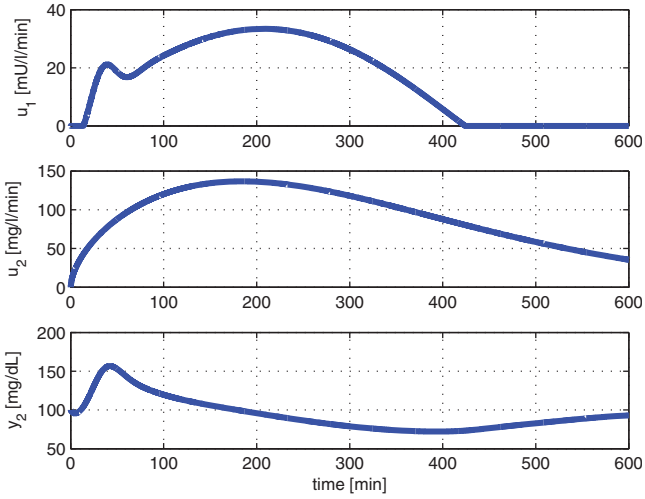

Figure 16. Closed-loop response of the nonlinear model with $p=[p_1 \;\; p_2 \;\; 1.5p_3]$.

Complex μ-controller synthesis has been used to formulate robust optimal glucose control problem. The selected control candidate has been designed to be robust against modeling uncertainties and fulfill performance requirements in a structured singular values sense. In comparison with the existing control methodology, the μ-control approach for T1DM regulation gives a less conservative control than the pure $\mathscr{H}_\infty$ one, in providing larger stability and performance margins. However, the price to pay reaching this goal is the increase of the controller dimension, but with computational power nowadays even a simulation of an approximately 40-dimensional LTI system is feasible. One of the weakness of the elaborated case study is certainly the lack of hard (e.g. control input) constraints. Unlike in model predictive control, the robust design methods suffer from application oriented but the theoretically correct handling of hard bounds. Recently in [48], a constrained $\mathscr{H}_\infty$ controller design for nonlinear systems is presented with special attention on real-time applications.

In this paper the novel Liu-Tang model [26] was analyzed. After transforming it to describe type 1 diabetes mellitus, a two degree-of-freedom controller structure was presented. The nonlinear model uncertainty was characterized by varying the model parameters and set up for controller design

DOI: 10.1002/oca

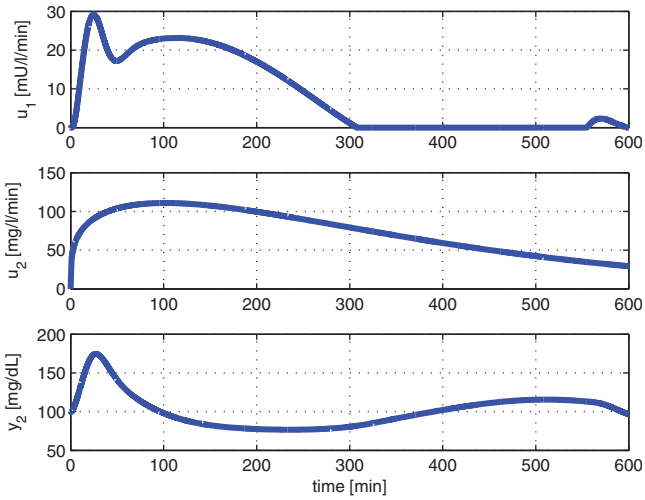

Figure 17. Closed-loop response of the nonlinear model with $p=[p_1 \;\; 0.8p_2 \;\; p_3]$.

by sensitivity analysis in frequency domain. Additional weighting functions were more restrictive than those presented in the literature. By the applied non-conservative complex μ-synthesis method not only RS is met under multiplicative uncertainty, but also the nominal performance, i.e. disturbance rejection is fulfilled. It was demonstrated (using glucose absorbtion scenario taken from the literature) that the controller tested on the original nonlinear model keeps blood glucose concentration in the desired range whereas the insulin amount to be injected is optimized.

Future research can be supported by the application of mixed uncertainties, nonlinear model-based robust control methods, model predictive control techniques, and different metabolic scenarios (e.g. physical activity, nocturnal hypoglycemia, long-term hyperglycemia).

ACKNOWLEDGEMENTS

The authors address special thanks to Dr Zsuzsanna Almássy from Heim Pál Children Hospital Budapest, Pediatric Department for her advices on diabetological questions. Moreover, the authors gratefully thank for the important and constructive comments of the unknown reviewers.

REFERENCES

1. Fonyó A, Ligeti E. Physiology (in Hungarian). *Medicina*: Budapest, 2008.
2. Wild S, Roglic G, Green A, Sicree R, King H. Global prevalence of diabetes—estimates for the year 2000 and projections for 2030. *Diabetes Care* 2004; **27**(5):1047–1053.
3. Jermendy G. Why is diabetes a problem? (in Hungarian). ENCOMPASS, Semester 8, Lecture 13, 2006.
4. Parker RS, Doyle III FJ, Ward JH, Peppas NA. Robust H_∞ glucose control in diabetes using a physiological model. *AIChE Journal* 2000; **46**(12):2537–2549.
5. Hernjak N, Doyle III FJ. Glucose control design using nonlinearity assessment techniques. *AIChE Journal* 2005; **51**(2):544–554.
6. Ruiz-Velazquez E, Femat R, Campos-Delgado DU. Blood glucose control for type I diabetes mellitus: a robust tracking H_∞ problem. *Control Engineering Practice* 2004; **12**:1179–1195.
7. Chee F, Fernando T. *Closed-loop Control of Blood Glucose*. Springer: Berlin, 2007.
8. Albisser AM. Insulin delivery systems: Do they need a glucose sensor? *Diabetes Care* 1982; **5**(3):166–173.
9. Furler SM, Kraegen EW, Smallwood RH, Chisolm DJ. Blood glucose control by intermittent loop closure in the basal mode: computer simulation studies with a diabetic model. *Diabetes Care* 1985; **8**(6):553–561.
10. Watts NB, Gebhart SSP, Clark RV, Phillips LS. Postoperative management of diabetes mellitus: steady-state glucose control with bedside algorithm for insulin adjustment. *Diabetes Care* 1987; **10**(6):722–728.
11. Chee F, Fernando T, van Heerden PV. Closed-loop glucose control in critically-ill patients using continuous glucose monitoring system (CGMS) in realtime. *IEEE Transactions on Information Technology in Biomedicine* 2003; **7**(1):43–53.
12. Marchetti G, Barolo M, Jovanovic L, Zisser H. An improved PID switching control strategy for type 1 diabetes. *Proceedings of the 28th IEEE EMBS Annual International Conference*, New York City, U.S.A., 2006; 5041–5044.

DOI: 10.1002/oca

13. Bolie VW. Coefficients of normal blood glucose regulation. *Journal of Applied Physiology* 1961; **16**(5):783–788.
14. Salzsieder E, Albrecht G, Fischer U, Freyse EJ. Kinetic modeling of glucoregulatory system to improve insulin therapy. *IEEE Transactions on Biomedical Engineering* 1985; **32**(10):846–855.
15. Bergman RN, Phillips LS, Cobelli C. Physiological evaluation of factors controlling glucose tolerance in man. *Journal of Clinical Investigation* 1981; **68**:1456–1467.
16. Candas B, Radziuk J. An adaptive plasma glucose controller based on a nonlinear insulin/glucose model. *IEEE Transactions on Biomedical Engineering* 1994; **41**(2):116–124.
17. De Gaetano A, Arino O. Mathematical modeling of the intravenous glucose tolerance test. *Journal of Mathematical Biology* 2000; **40**:136–168.
18. Cobelli C, Mari A. Control of diabetes with artificial systems for insulin delivery—algorithm independent limitations revealed by a modeling study. *IEEE Transactions on Biomedical Engineering* 1985; **32**(10):840–845.
19. Hovorka R, Shojaee-Moradie F, Carroll PV, Chassin LJ, Gowrie IJ, Jackson NC, Tudor RS, Umpleby AM, Jones RH. Partitioning glucose distribution/transport, disposal and endogenous production during IVGTT. *American Journal of Physiology*, *Endocrinology and Metabolism* 2002; **282**:992–1007.
20. Hovorka R, Canonico V, Chassin LJ, Haueter U, Massi-Benedetti M, Federici MO, Pieber TR, Schaller HC, Schaupp L, Vering T, Wilinska ME. Nonlinear model predictive control of glucose concentration in subjects with type 1 diabetes. *Physiological Measurement* 2004; **25**:905–920.
21. Kovács L, Paláncz B. Glucose-insulin control of Type 1 diabetic patients in $\mathscr{H}_2/\mathscr{H}_\infty$ space via computer algebra. *Proceedings of the Second International Conference on Algebraic Biology*, Austria. Lecture Notes in Computer Science, vol. 4545. Springer: Berlin, 2007; 95–109.
22. Kovács L, Kulcsár B, Benyó B, Benyó Z. Induced L_2-norm minimization of glucose-insulin system for type I diabetic patients. *Seventh IFAC Symposium on Modelling and Control in Biomedical Systems*, Aalborg, Denmark, 2009; 55–60.
23. Femat R, Ruiz-Velazquez E, Quiroz G. Weighting restriction for intravenous insulin delivery on T1DM patient via $\mathscr{H}_\infty$ control. *IEEE Transactions on Automation and Engineering* 2009; **6**(2):239–247.
24. Carson ER, Cobelli C, Finkelstein L. The mathematical modelling of metabolic and endocrine systems—model formulation, identification and validation. *Biomedical Engineering and Health Systems*. Wiley: New York, 1983.
25. Cherruault Y. *Mathematical Modelling in Biomedicine*. D. Reidel Publishing Company: Dordrecht, Holland, 1986.
26. Liu W, Tang F. Modeling a simplified regulatory system of blood glucose at molecular levels. *Journal of Theoretical Biology* 2008; **252**:608–620.
27. Sorensen JT. A Physiologic model of glucose metabolism in man and its use to design and assess improved insulin therapies for diabetes. *Ph.D. Dissertation*, Massachusetts Institute of Technology, 1985.
28. Bergman RN, Finegood DT, Ader M. Assessment of insulin sensitivity in vivo. *Endocrine Reviews* 1985; **6**:45–86.
29. Sturis J, Polonsky KS, Mosekilde E, Cauter EV. Computer model for mechanisms underlying ultradian oscillations of insulin and glucose. *American Journal of Physiology*, *Endocrinology and Metabolism* 1991; **260**:801–809.
30. Turner RC, Holman RR, Matthews D, Hockaday TD, Peto J. Insulin deficiency and insulin resistance interaction in diabetes: estimation of their relative contribution by feedback analysis from basal plasma insulin and glucose concentrations. *Metabolism* 1979; **28**(11):1086–1096.
31. Rizza RA, Mandarino LJ, Gerich JE. Dose-response characteristics for effects of insulin on production and utilization of glucose in man. *American Journal of Physiology*, *Endocrinology and Metabolism* 1981; **240**: 630–639.
32. Korach-André M, Roth H, Barnoud D, Péan M, Péronnet F, Leverve X. Glucose appearance in the peripheral circulation and liver glucose output in men after a large 13C starch meal. *American Journal of Clinical Nutrition* 2004; **80**:881–886.
33. Galgani J, Aguirre C, Diaz E. Acute effect of meal glycemic index and glycemic load on blood glucose and insulin responses in humans. *Nutrition Journal* 2006; **5**:22.
34. Wong XW, Chase JG, Hann CE, Lotz TF, Lin J, Le Compte AJ, Shaw GM. In silico simulation of long-term type 1 diabetes glycemic control treatment outcomes. *Journal of Diabetes Science and Technology* 2008; **2**(3):436–449.
35. György A. The novel molecular model of the human blood glucose system from the aspect of control theory. *Master's Thesis*, Budapest University of Technology and Economics, 2009.
36. Kovács L, György A, Almassy Zs, Benyó Z. Analyzing a novel model of human blood glucose system at molecular levels. *European Control Conference*, Budapest, Hungary, 2009; 2494–2499.
37. Isidori A. *Nonlinear Control Systems*. Springer: Berlin, 1995.
38. Hangos KM, Bokor J, Szederkenyi G. *Analysis and Control of Nonlinear Process Systems*. Springer: Berlin, 2004.
39. Lantos B. *Theory and Design of Control Systems I–II* (*in Hungarian*). Akademia: Budapest, 2001.
40. Willcox K, Peraire J. Balanced model reduction via the proper orthogonal decomposition. *AIAA Journal* 2002; **40**(11):2323–2330.
41. Doyle JC, Glover K, Khargonekar PP, Francis BA. State-space solutions to standard $\mathscr{H}_2$ and $\mathscr{H}_\infty$ control problems. *IEEE Transactions on Automatic Control* 1996; **34**(8):831–847.
42. Zhou K. *Robust and Optimal Control*. Prentice-Hall: New Jersey, 1996.
43. Balas GJ, Doyle JC, Glover K, Packard A, Smith R. μ *Analysis and Synthesis Toolbox*. MUSYN Inc. and The Mathworks Inc., 1991.

DOI: 10.1002/oca

44. Kovács L. New principles and adequate control methods for insulin dosage in case of diabetes (in Hungarian). *Ph.D. Thesis*, Budapest University of Technology and Economics, Department of Electrical Engineering and Informatics, 2007.
45. Gu DW, Petkov PH, Konstantinov MM. *Robust Control Design with MATLAB*. Springer: London, 2005.
46. Quiroz G, Femat R. On hyperglycemic glucose basal levels in tpye 1 diabetes mellitus from dynamic analysis. *Mathematical Biosciences* 2007; **210**(5):554–575.
47. Piotrovskii VK. The use of Weibull distribution to describe the in vivo absorption kinetics. *Journal of Pharmacokinetics and Pharmacodynamics* 1987; **15**(6):681–686.
48. Péni T, Kulcsár B, Bokor J. Induced L_2 norm improvement by interpolating controllers for dicrete time LPV systems. *European Journal of Control* 2009; **15**:545–559.

DOI: 10.1002/oca